PERGAMON

International Journal of Heat and Mass Transfer 45 (2002) 1109–1116

International Journal of HEAT and MASS TRANSFER

www.elsevier.com/locate/ijhmt

Morphology of soot collected in microgravity droplet flames

Samuel L. Manzello [a,1], Mun Y. Choi [b,*]

[a] *Department of Mechanical Engineering, University of Illinois at Chicago, Chicago, IL 60607, USA*
[b] *Department of Mechanical Engineering and Mechanics, Drexel University, Philadelphia, PA 19104, USA*

Received 16 March 2000; received in revised form 14 April 2001

Abstract

Measurements of the primary particle size, radius of gyration, fractal dimension, and the mass fractal prefactor were measured for soot sampled in *n*-heptane droplet flames under microgravity conditions. These represent the first such measurements obtained for spherically symmetric droplet flames. Experiments were performed in the NASA-Glenn Research Center in Cleveland, OH. Soot was sampled at 0.2 and 0.5 s after ignition for a 2.1 mm droplet burning in atmospheric pressure air. The measured primary particle sizes were significantly larger under microgravity conditions compared to normal gravity and were found to increase with residence time. The average radius of gyrations were also larger for soot collected in microgravity conditions. Differences in the particle and agglomerate dimensions are believed to be caused by the longer residence times. The fractal dimensions were found to be nearly constant for all experiments while the prefactor term was found to increase slightly with residence time. © 2002 Elsevier Science Ltd. All rights reserved.

Keywords: Soot; Fractal properties; Microgravity; Droplet combustion

1. Introduction

Soot is a common by-product resulting from combustion of fossil fuels. Release of soot into the atmosphere contributes to environmental and health hazards including the degradation of atmospheric visibility, ground-water contamination, and premature deaths due to ingestion. Sooting can also decrease the efficiency of energy conversion systems since carbonaceous particulates represent incomplete combustion and can cause hardware fouling. The importance of these topics has fueled numerous fundamental investigations of soot processes under normal-gravity conditions [1–5]. However, buoyancy-induced flows in normal-gravity flames produce short residence times to resolve soot formation, growth, agglomeration, and oxidation processes. Recent experiments using microgravity environments have produced longer residence times (by as much as three times for laminar gas-jet diffusion flames) and expanded the soot containing region to allow for accurate resolution of the soot evolution processes and for reliable soot diagnostics [6–9].

Sooting in microgravity environments present unique opportunities to investigate important mechanisms that are normally obscured under normal-gravity conditions. For example, the absence of convective flows in microgravity enables radiation as an important mode of heat transfer. Since radiation from carbonaceous particulates is much greater than from non-luminous radiation (attributed to gas species), the importance of sooting is further amplified in reduced-gravity [10]. Under microgravity conditions, sooting effects that were deemed negligible, based on normal-gravity observations, were observed to be enhanced [11]. For example, the measurements of soot concentrations for microgravity droplet flames were an order of magnitude larger than the counterpart normal-gravity flames [12]. The high soot concentrations were responsible for a greater degree of radiative heat losses and contributed to the reduction in the droplet burning rate [13,14]. Investiga-

* Corresponding author. Tel.: +1-215-895-6984; fax: +1-215-895-4929.
E-mail address: Choi@Drexel.edu (M.Y. Choi).
[1] NRC-NIST Post Doctoral Fellow.

PII: S0017-9310(01)00164-8

Nomenclature

A_a	projected area of agglomerate
A_p	projected area of primary particle
d_p	diameter of the soot primary particle
D_f	fractal dimension
d_0	initial droplet diameter
k_f	mass fractal prefactor
K	droplet burning rate
N	number of primary particles
r_c	centroid of agglomerate
r_d	instantaneous droplet radius
r_f	instantaneous flame radius
r_i	centroid of primary particle
R_g	radius of gyration
t_b	droplet burning time

tion of spherically-symmetric acetylene/air diffusion flames supported on a porous sphere burner indicated that sooting can promote the onset of flame extinction [15]. However, despite the importance of the morphological properties of soot in the interpretation of the soot processes, there has been a lack of measurements in spherically-symmetric diffusion flames.

Characterization of soot morphological properties including the primary particle size, d_p, radius of gyration, R_g, fractal dimension, D_f, and mass fractal prefactor term, k_f are important for the analysis of soot processes including primary particle growth, soot agglomeration and oxidation processes. Morphological measurements are also required for accurate formulation of optical properties (including the absorption, emission and scattering constants [16]) for flame radiative emission calculations and in the interpretation of soot optical diagnostics measurements [17].

Ku et al. [7] and Konsur et al. [8] were the first to thermophoretically sample soot in microgravity laminar gas jet diffusion flames. The soot sampled from ethylene and propane flames was analyzed using transmission electron microscopy (TEM) for primary particle size and agglomerate dimensions. The average primary particle diameter was found to be a factor of two larger under microgravity conditions compared to normal-gravity measurements. The longer residence time in microgravity enhanced the soot formation and growth processes [7]. Urban et al. [9] also recently sampled soot from microgravity laminar jet diffusion flames in experiments aboard the space shuttle. Similar trends of larger soot primary sizes for microgravity flames were observed.

Although the microgravity findings [7–9] provided important and useful information regarding the morphology of soot collected in laminar diffusion flames in microgravity, their results are not directly transferable for analysis of soot properties of microgravity droplet combustion. There are significant differences in the residence times between the two cases. In microgravity droplet combustion, the vaporized fuel is diffused toward the flame front while undergoing pyrolysis reactions to form precursors that evolve into carbonaceous soot. Once formed near the high-temperature region, the soot is acted upon by thermophoresis and transported towards the droplet. Opposing this mode of particle transport is the viscous drag caused by the Stefan flux (due to the vaporizing fuel droplet). The soot agglomerates ultimately reside at a radial position where these two forces are in balance, namely the sootshell location, which occurs at a non-dimensional radius (r_s/r_d) of approximately 3. Sootshells are typically observed to form within 0.1 s after ignition and linger throughout the burning lifetime. Thus, the residence time scales approximately as the square of the initial droplet diameter since the burning time ($t_b = d_0^2/K$) is proportional to the square of the initial droplet diameter. For a droplet of 2 mm diameter, the residence time is ~6–8 s depending on the burning rate. In contrast, the residence time for a typical microgravity laminar gas-jet diffusion flame is approximately 100 ms [9]. Spherically symmetric flames produced under microgravity also provide a unique geometrical configuration in which to study sooting processes since the transport mechanisms of thermophoresis, diffusion, and viscous drag can be formulated using a one-dimensional model. The motivation for the present study is to sample soot within the sootshell of a *n*-heptane flame under microgravity conditions to investigate the influence of residence time on soot morphology. Morphological measurements including d_p, R_g, D_f, and k_f for soot collected in microgravity droplet flames are compared to normal-gravity results.

2. Experimental apparatus and procedures

The microgravity experiments were performed in the NASA-Glenn Research Center 2.2 s droptower in Cleveland, OH (see Fig. 1). Microgravity conditions are produced for 2.2 s by releasing the experimental rig into free-fall within the eight story structure. The impact of the experiment at the bottom of the tower is reduced by using a large airbag system. The experimental rig is designed to investigate the influences of sooting on droplet combustion [14]. Fig. 2 is a schematic of the experimental rig including the 12 liter stainless steel combustion chamber. The combustion chamber contains the fuel delivery system, droplet generator, and the ignition

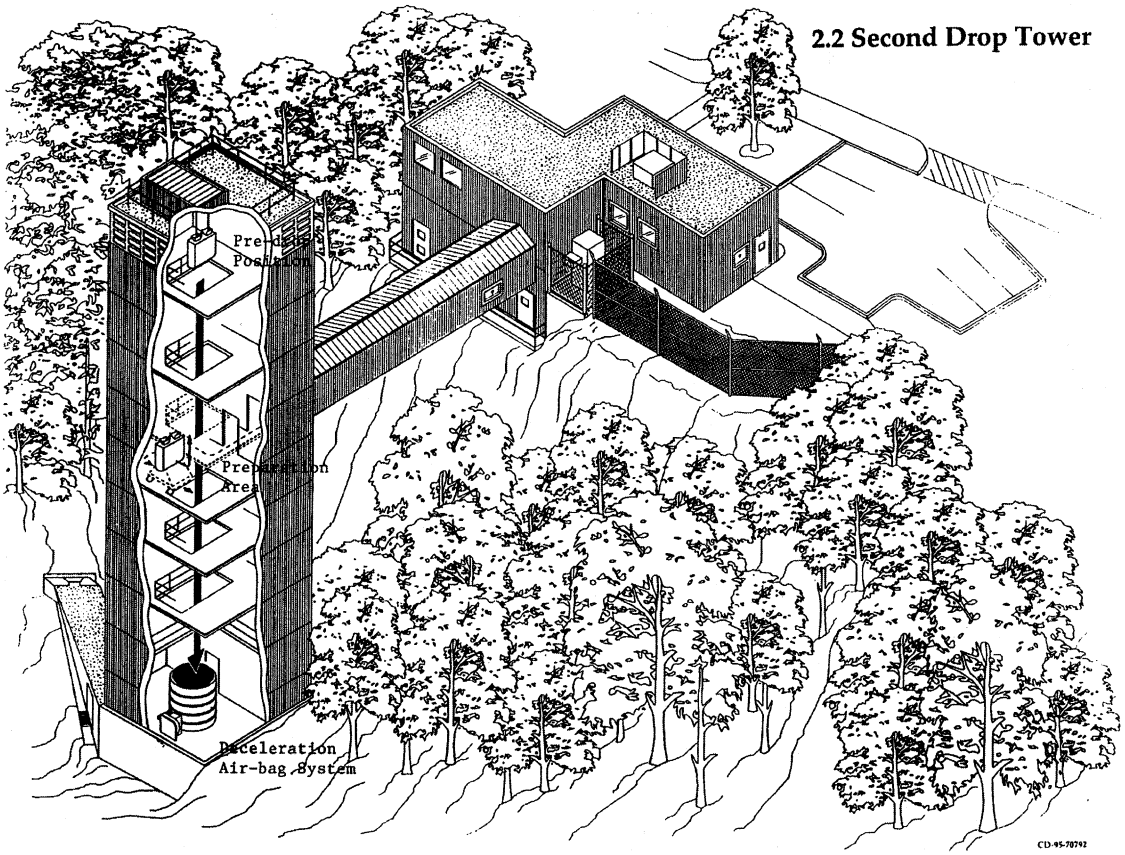

Fig. 1. Schematic of the NASA Glenn 2.2 s droptower facility.

assembly. The fuel droplets are generated using two opposed hypodermic needles of 0.25 mm diameter that are separated by 0.5 mm prior to the initiation of the experiment. Fuel is pumped through the needles by solenoid-activated syringes attached to each needle. Each hypodermic needle is attached to a separate rotating galvanometric device. The exiting fuel forms a liquid bridge and the rapid rotation of the needles in opposite direction deposits the droplet onto a 15 μm SiC fiber. The fiber is used to fix the location of the droplet and prevent the droplet from moving out of the field of view. Approximately 0.2 s after deployment of the droplet, the fuel droplet is ignited by two hot wire igniters placed symmetrically about the droplet.

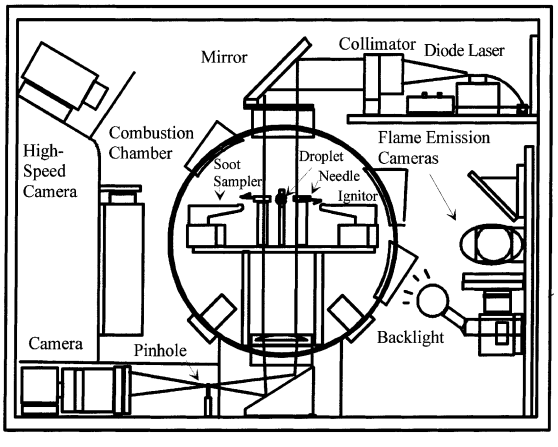

Fig. 2. Schematic of microgravity droplet combustion experimental apparatus.

Soot agglomerates within the flame were sampled employing a thermophoretic deposition method. The sampling assembly consisted of a single-axis linear stepper motor (Northern Magnetics, model number 0602-2) which was controlled using an IMS motion controller (model number IM483I2). The linear stepper motor was programmed prior to each experiment for motor acceleration, velocity and sampling duration to minimize the disturbance to the droplet. A holder designed to accommodate copper TEM grids (3 mm in diameter, 300 mesh with a carbon substrate, Ted Pella, part number 01820) was attached to the linear motor.

The entire sampling procedure was imaged using a laser back-lit view (normally used for soot light extinction measurements) in tandem with a high speed camera operated at 200 frames per second (which was illuminated using an incandescent backlight). For the laser back-lit view, light from a 635 nm diode laser attached to a single fiber optic cable was expanded to a diameter of 50 mm. The beam was collimated and directed through the top optical port of the combustion chamber, focused using a 200 mm focal length plano-convex lens and reflected using a second mirror positioned at 45°. The reflected beam was then imaged through a spatial filter to a high resolution CCD camera and recorded on a Betacam recorder through a fiber optic coupler.

Soot sampling was performed at 0.2 and 0.5 s after ignition for two separate microgravity experiments, to determine the influence of residence time on the soot morphology. Fig. 3 shows a schematic of the soot sampling apparatus and the microgravity droplet flame. The sampling probe insertion time through the flame was measured to be approximately 0.1 s (the retraction time was the same). The sampling probe dwell time within the sootshell was approximately 0.2 s.

Soot agglomerates were imaged using a JEOL TEM operated at 50 K for the normal-gravity soot and at 26 and 50 K for the microgravity soot. Fig. 4 displays images of soot agglomerates obtained from the normal-gravity flame and for the microgravity flame at 0.5 s after ignition. The micrographs obtained from the TEM analysis were placed on a light table and imaged using a high-resolution CCD camera with a 18-108 mm lens. The images were then digitized using a 480×512, 8 bit graylevel resolution Data Translation DT-2851 frame grabber board and a DT-2858 co-processor. The attached 18-108 zoom lens allowed further magnification of the image required for primary particle diameter measurements. Spatial calibration was obtained by using a separate TEM grid deposited with 100 nm polystyrene spheres. After the determination of a threshold (based on image enhancing technique [18]), the primary particle sizes were measured using manual edge identification [19]. The radius of gyration was measured using an automated image processing algorithm developed in the author's laboratory which is described in the next section.

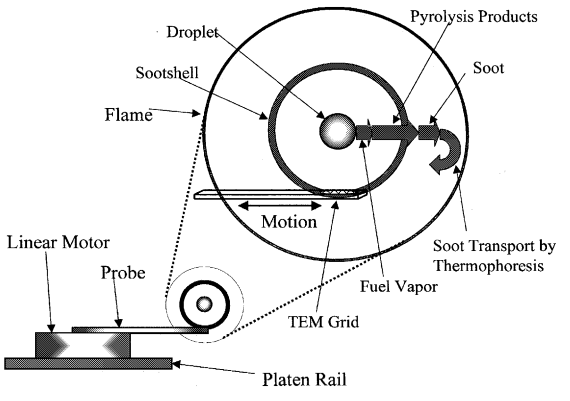

Fig. 3. Schematic of sampling apparatus, and of a microgravity droplet flame including the sootshell.

3. Results and discussion

The histogram distribution of the primary particle size measurements for all three experiments are displayed in Figs. 5(a)–(c). Approximately 200 particles were analyzed for each experiment. The average primary particle size increased from 25.9 nm in normal gravity to 38.5 nm and 45.8 nm for the 0.2 and 0.5 s microgravity experiments (see Table 1). The increase in the primary particle dimensions with residence time is dramatic. For example, the volume of an average primary particle is nearly 70% larger for the 0.5 s case compared to the 0.2 s case. The increase in the primary particle size between normal gravity and microgravity are in qualitative agreement with soot sampled in laminar jet diffusion flames in microgravity [7,9]. At a height above burner of 10 mm, Ku et al. [7] found that the primary particle diameter of ethylene increased from 20 nm in normal gravity to 38 nm in microgravity. The increase in primary particle size is due to the increased residence time afforded by microgravity environments. However, there are important differences between the two geometries of the laminar gas-jet and the spherically-symmetric droplet flames. For the laminar gas-jet flames, residence time is dependent on the height above burner. Furthermore, measurements of Ku et al. [7] clearly demonstrate that there are operating conditions in microgravity which demonstrate the formation, growth and oxidation processes.These observations are not likely to occur in droplet combustion configurations since soot resides within the sootshell, far removed from the regions where oxidizers are present in appreciable concentrations [20].

Avedisian [21] performed soot primary particle measurements for toluene droplet flames in microgravity. In their experiments, soot was deposited on filter paper (placed at various locations on the combustion chamber) due to the impact of the experiment with the ground. Subsequent TEM analysis was performed to measure the primary particle diameters (average $d_p \sim 50$ nm). Since the technique neither provided temporal nor spatial information regarding the collected soot, the influence of residence times on soot morphology could not be inferred. In that study, agglomerate properties such as the radius of gyration, fractal dimension, and the mass fractal dimension were not measured.

The measurements of the radius of gyration in this study are used primarily to determine the fractal

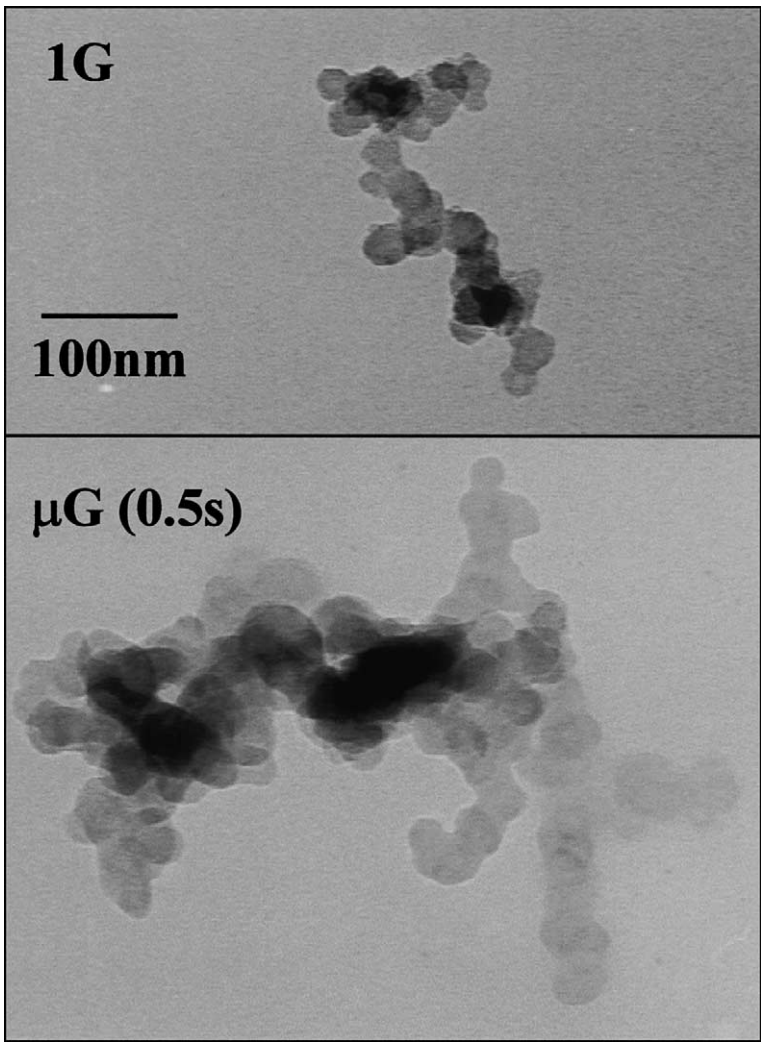

Fig. 4. Transmission electron micrograph images of soot agglomerates in normal gravity and in microgravity (0.5 s after ignition).

Table 1

Experiment	d_p (nm) [S.D.]	R_g (nm) [S.D.]	Range of R_g (nm)	D_f	k_f
Normal gravity	25.9 [4.8]	46.4 [22.7]	15–130	1.59	6.5
μg 0.2 s After ignition	38.5 [7.9]	80.0 [33.2]	28–204	1.56	7.0
μg 0.5 s After ignition	45.8 [8.1]	115.6 [49.4]	37–270	1.61	7.6

dimension and to offer insights regarding the relative differences in agglomerate sizes for the three cases. In mass fractal analysis, the number of primary particles, N, comprising an agglomerate and soot dimensions are related by the following equation [22]:

$$N = k_f \left(\frac{R_g}{d_p} \right)^{D_f}, \quad (1)$$

where D_f is the fractal dimension and k_f is the prefactor term. The measurements of D_f and k_f can provide important insights regarding the agglomerate growth mechanisms [4]. These parameters can be calculated based on the measurement of N, R_g, and d_p. In this study, the number of primary particles per agglomerate was calculated by measuring the projected area of the

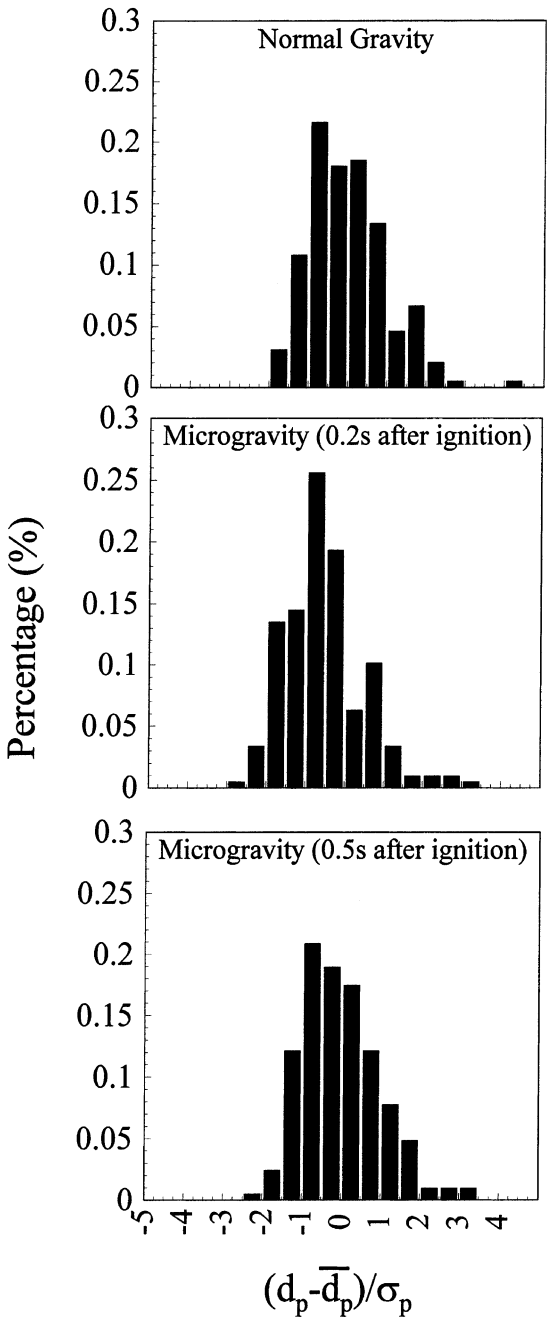

Fig. 5. Normalized histogram distributions for primary particle size measurements for normal gravity, 0.2 s microgravity, and 0.5 s microgravity experiments.

agglomerate, A_a, and the projected area of the primary particle, A_p (based on mean d_p measurements)

$$N = 1.0\left(\frac{A_a}{A_p}\right)^{1.08}. \tag{2}$$

The radius of gyration based on the projected image of the agglomerate was measured using a custom-image processing algorithm. The radius of gyration of an agglomerate is defined by the following relationship:

$$R_g = \sqrt{\sum_{i=1}^{N} \frac{(r_i - r_c)^2}{N}}, \tag{3}$$

where r_i is the centroid of the primary particle and r_c is the centroid of the agglomerate. Since it is difficult to identify each individual particle that constitute an agglomerate (due to the sheer number of particles concerned which can range from a few to a few thousands), the R_g calculation formulation was revised by considering each pixel to be the individual element of interest [22]. The equation for the radius of gyration remains the same but N now corresponds to the total number of pixel elements comprising the agglomerate (typically on the order of 20–30 thousand pixels in our experiments).

The average R_g for the normal-gravity experiment was 46.4 nm (based on 92 agglomerates) whereas for the 0.2 and 0.5 s microgravity experiments, values of 80.0 nm (146 agglomerates) and 115.6 nm (119 agglomerates) were measured, respectively. This increase is a manifestation of the extended residence time (due to influence of thermophoresis in 'trapping soot' within the sootshell) during which additional growth and agglomeration can occur. The differences among the experiments are not only apparent when comparing the mean values but also in the ranges of agglomerate sizes measured. The ranges in R_g for the normal gravity, 0.2 and 0.5 s cases are 15–130, 28–204, 37–270 nm, respectively. Since the transport of soot agglomerates formed near the high-temperature region towards the sootshell occurs throughout the burning lifetime, the agglomerates within the sootshell should display wider distribution of newly formed and mature soot of varying age as residence time increases.

The measurements of N, R_g for each agglomerate and the average value of d_p for each condition were used to calculate D_f and k_f. As shown in Figs. 6(a)–(c) (for measurements obtained in normal gravity, 0.2 s microgravity, and 0.5 s microgravity), the fractal dimension represents the slope of the $\ln[N]$ versus $\ln[R_g/d_p]$ and the prefactor term is the intercept at $R_g = d_p$. These results are also summarized in Table 1. Unlike the physical dimension measurements, D_f was nearly constant for all three cases. D_f for normal-gravity soot was 1.59, whereas for the 0.2 and 0.5 s, cases they were 1.56 and 1.61, respectively. The fractal dimensions for the three cases are consistent with previous normal-gravity results obtained for gaseous (acetylene, propylene, ethylene, propane) turbulent diffusion flames [23]. In that study, it was found that the average D_f (measured using similar approach as described in the present study) was approximately 1.65 [23]. The investigation of Ku et al.

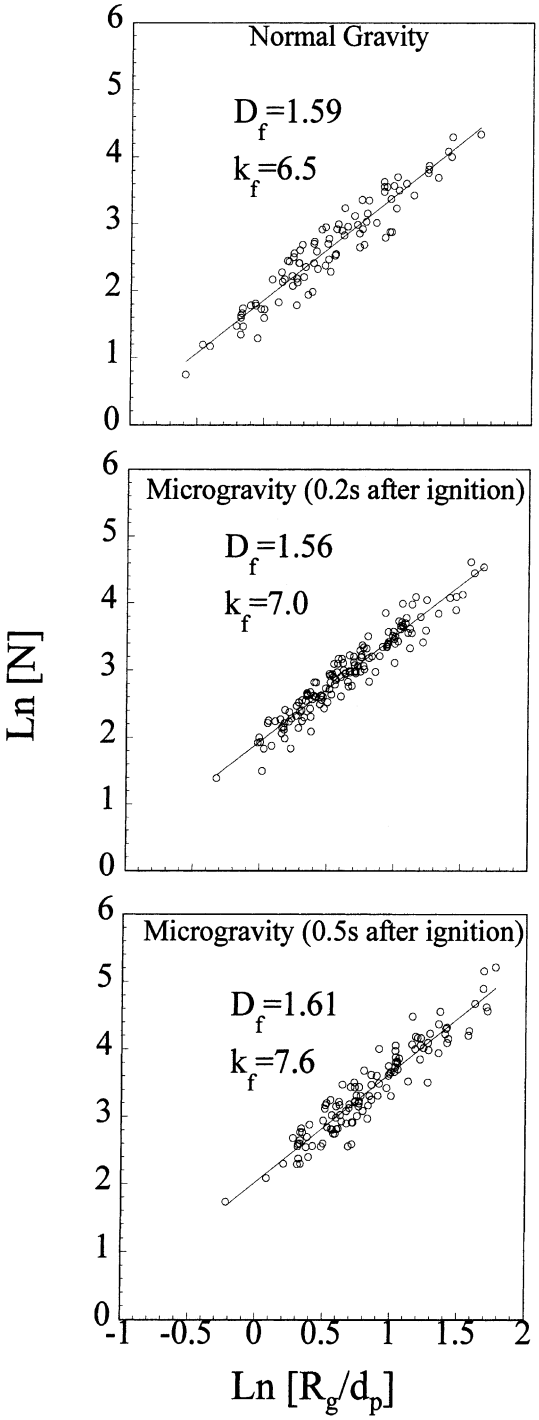

Fig. 6. Plot of $\ln[N]$ versus $\ln[R_g/d_p]$ for soot measurements in normal gravity, 0.2 s microgravity, and 0.5 s microgravity experiments.

[7] is the only other study for which fractal dimensions were measured for soot produced in microgravity diffusion flames. Ku et al. [7] measured the fractal dimension for ethylene and propane that ranged from 1.41 to 1.93.

The prefactor term, in addition to the fractal dimension, is essential for the accurate characterization of the soot morphology and the agglomeration process [24]. The magnitude of the prefactor term represents the compactness, i.e., the level of packing of the soot primary particles that comprise the agglomerate [25]. In our experiments, the average k_f increased slightly from 6.5 in normal gravity to 7.0 and 7.6 for the 0.2 and 0.5 s microgravity experiments, respectively. The increase in the number of primary particles comprising an agglomerate scales linearly with k_f. There are no other measurements of k_f (based on R_g) for soot collected in microgravity flames. The present values are, however, within the reported measurements of k_f for normal-gravity experiments which range from approximately 4.0 for soot collected in a laminar premixed flame [24] to 8.5 for soot collected in the overfire region of turbulent diffusion flames [23]. Additional experiments will be required to fully investigate this behavior.

These experiments have demonstrated that the morphological properties of soot produced in microgravity droplet flames are significantly different than those measured in normal-gravity experiments. Furthermore, the spherically-symmetric droplet configuration is unique in that the residence time can be controlled over a range beyond what can be obtained for laminar gas-jet diffusion flames. Additional experiments using facilities producing longer microgravity observation times are required to investigate whether the observed trends of the soot physical and fractal dimensions continue with increasing residence times.

Acknowledgements

The authors gratefully acknowledge support through NASA (NCC3-655 and NCC3-822, Dr. Paul Ferkul serving as project scientist). S.L.M. also acknowledges support from a NASA GSRP fellowship. The assistance of the NASA-GRC staff (Messrs. A. Birchenough, M. Johnston, R. Mileto, C. Hampton, J. Carrion and J. Owens) is sincerely appreciated.

References

[1] R.J. Santoro, T. Yeh, T.T. Horvath, The transport and growth of soot particles in laminar diffusion flames, Combust. Sci. Technol. 53 (1987) 89–115.

[2] S.J. Harris, A.M. Weiner, Surface growth of soot particles in premixed ethylene/air flames, Combust. Sci. Technol. 31 (1983) 155–167.

[3] A. D'Alessio, Laser light scattering and fluorescence diagnostics of rich flames produced by gaseous and liquid

fuels, in: D. Siegla, G. Smith (Eds.), Particulate Carbon, Formation during Combustion, Plenum Press, New York, 1981.
[4] C.M. Megaridis, R.A. Dobbins, Morphological description of flame-generated materials, Combust. Sci. Technol. 71 (1990) 95–109.
[5] J. Zhang, C.M. Megaridis, Soot microstructure in steady and flickering laminar methane/air diffusion flames, Combust. Flame 112 (1998) 473–484.
[6] C.K. Law, G.M. Faeth, Opportunities and challenges of combustion in microgravity, Prog. Energy Combust. Sci. 20 (1994) 65–113.
[7] J.C. Ku, D.W. Griffin, P.S. Greenberg, J. Roma, Buoyancy-induced differences in soot morphology, Combust. Flame 102 (1995) 216–218.
[8] B. Konsur, C.M. Megaridis, D. Griffin, Fuel preheat effects on soot-field structure in laminar gas jet diffusion flames burning in 0-G and 1-G, Combust. Flame 116 (1999) 334–347.
[9] D.L. Urban, Z.G. Yuan, P.B. Sunderland, G.T. Linteris, J.E. Voss, K.C. Lin, Z. Dai, K. Sun, G.M. Faeth, Structure and soot properties of non-buoyant ethylene/air laminar jet diffusion flames, AIAA J. (1998) 1346–1360.
[10] R. Siegel, J. Howell, Thermal Radiation Heat Transfer, third ed., Hemisphere, New York, 1981.
[11] B.D. Shaw, F.L. Dryer, F.L. Williams, J.B. Haggard Jr., Sooting and disruption in spherically-symmetrical combustion of decane in air, Acta Astron. 17 (1988) 1195–1202.
[12] M.Y. Choi, K.O. Lee, Investigation of sooting in microgravity droplet combustion, Proc. Combust. Inst. 26 (1996) 1149–1153.
[13] G.S. Jackson, C.T. Avedisian, The effect of initial droplet diameter in spherically symmetric droplet combustion of sooting fuels, Proc. R. Soc. London A 446 (1994) 255–276.
[14] K.O. Lee, S.L. Manzello, M.Y. Choi, The effects of initial diameter on sooting and burning behavior of isolated droplets under microgravity conditions, Combust. Sci. Technol. 132 (1998) 139–156.
[15] S. Berhan, A. Atreya, D. Everest, Radiant extinction of gaseous diffusion flames, in: Proceedings of the Fifth International Microgravity Combustion Workshop, NASA/CP 208917, Cleveland, OH, 1999, pp. 43–46.
[16] R.A. Dobbins, G.W. Mulholland, N.P. Bryner, Comparison of a fractal smoke optics model with light extinction measurements, Atmos. Environ. 28 (1994) 873–887.
[17] Ü.Ö. Köylü, G.M. Faeth, Structure of overfire soot in buoyant turbulent diffusion flames at long residence times, Combust. Flame 89 (1992) 140–156.
[18] M.Y. Choi, Droplet combustion characteristics under microgravity and normal gravity conditions, Ph.D. Thesis, Princeton University, 1992.
[19] J. Zhang, The influence of ferrocene additive on soot formation in laminar ethylene diffusion flames, Ph.D. Thesis, University of Illinois, Chicago, 1995.
[20] A.J. Marchese, F.L. Dryer, V. Nayagam, Numerical modeling of isolated *n*-alkane droplet flames: initial comparisons with ground and space-based microgravity experiments, Combust. Flame 116 (1999) 432–459.
[21] C.T. Avedisian, Soot formation in spherically symmetric droplet combustion, in: F.L. Dryer, R.F. Sawyer (Eds.), Physical and Chemical Aspects of Combustion, Gordon and Breach, New York, 1996, pp. 135–160.
[22] R. Jullien, R. Botet, Aggregation and Fractal Aggregates, World Scientific, New York, 1987.
[23] Ü.Ö. Köylü, G.M. Faeth, T.L. Farias, M.G. Carvalho, Fractal and projected structure properties of soot aggregates, Combust. Flame 100 (1995) 621–633.
[24] J. Cai, N. Lu, C. Sorensen, Analyis of fractal cluster morphology parameters: structural coefficient and density autocorrelation function cutoff, J. Colloid Interface Sci. 171 (1995) 470–473.
[25] S. Wu, S.K. Friedlander, Note on the power law equation for fractal-like aerosol agglomerates, J. Colloid Interface Sci. 159 (1993) 246–248.